Supplemental Material: Momentum-resolved lattice dynamics of parent and electron-doped Sr_2IrO_4

C. D. Dashwood,[1,*] H. Miao,[2] J. G. Vale,[1] D. Ishikawa,[3] D. A. Prishchenko,[4] V. V. Mazurenko,[4] V. G. Mazurenko,[4] R. S. Perry,[1] G. Cao,[5] A. de la Torre,[6,7] F. Baumberger,[7] A. Q. R. Baron,[3] D. F. McMorrow,[1] and M. P. M. Dean[2]

[1]*London Centre for Nanotechnology and Department of Physics and Astronomy, University College London, Gower Street, London WC1E 6BT, UK*

[2]*Department of Condensed Matter Physics and Materials Science, Brookhaven National Laboratory, Upton, New York 11973, USA*

[3]*Materials Dynamics Laboratory, RIKEN SPring-8 Center, RIKEN, Sayo Hyogo 697-5148, Japan*

[4]*Department of Theoretical Physics and Applied Mathematics, Ural Federal University, 19 Mira Street, Ekaterinburg 620002, Russia*

[5]*Department of Physics, University of Colorado at Boulder, Boulder, Colorado 80309, USA*

[6]*Institute for Quantum Information and Matter and Department of Physics, California Institute of Technology, Pasadena, California 91125, USA*

[7]*Department of Quantum Matter Physics, University of Geneva, 24 Quai Ernest-Ansermet, 1211 Geneva 4, Switzerland*

(Dated: August 2, 2019)

I. DYNAMIC STRUCTURE FACTOR CALCULATIONS

The intensity measured in non-resonant inelastic x-ray scattering (IXS) at total momentum transfer $\mathbf{Q}$ and energy loss ω is directly proportional to the dynamic structure factor $S(\mathbf{Q},\omega)$, with the constant of proportionality depending on the momenta and polarisation of the incoming/outgoing photons[1]. Away from Bragg reflections, $S(\mathbf{Q},\omega)$ is dominated by the one-phonon term, which in the Born approximation reads

$$S(\mathbf{Q},\omega) = \sum_{q,j} |F(\mathbf{Q},\mathbf{q},j)|^2 \langle n_{qj}+1\rangle \delta(\omega-\omega_{qj})\delta(\mathbf{Q}-\mathbf{q}) \tag{S1}$$

where $\mathbf{q}$ sums over the reduced momenta in the first Brillouin zone, and j sums over the $3n$ modes at $\mathbf{q}$ (n being the number of atoms in the primitive unit cell) with frequencies ω_{qj} and Bose factors $\langle n_{qj}+1\rangle = \left(1-e^{-\omega_{qj}/(k_bT)}\right)^{-1}$. F is given by

$$F(\mathbf{Q},\mathbf{q},j) = \sum_d \sqrt{\frac{f_d(\mathbf{Q})}{2m_d\omega_{qj}}} e^{-W_d(\mathbf{Q})} e^{-\imath\mathbf{Q}\cdot\mathbf{r}_d} \mathbf{Q}\cdot\mathbf{e}_{qjd} \tag{S2}$$

where d sums over the n atoms in the primitive unit cell with masses m_d located at $\mathbf{r}_d$, $e^{-W_d(\mathbf{Q})}$ is the Debye-Waller factor, $\mathbf{e}_{qjd}$ the complex phonon polarisation, and $f_d(\mathbf{Q})$ the x-ray form factor.

Equation S1 was evaluated using the PHONOPY package[2]. In order to be directly compared with our IXS data, however, a finite linewidth γ_{qj} (due mostly to instrument resolution) must be introduced by replacing the frequency delta function with a damped harmonic oscillator lineshape

$$\delta(\omega-\omega_{qj}) \to \chi''_j(\mathbf{q},\omega) = \frac{4\omega\omega_{qj}\gamma_{qj}}{\pi\left[\left(\omega^2-\omega_{qj}^2-\gamma_{qj}^2\right)^2+4\omega^2\gamma_{qj}^2\right]}. \tag{S3}$$

We use $\gamma_{qj} = \gamma = 0.8\,\text{meV}$ for all modes at all momenta.

II. SPACE GROUP COMPARISON

Neutron diffraction[3,4] and nonlinear optical experiments[5] have shown the true space group of Sr_2IrO_4 to be $I4_1/a$. The difference from $I4_1/acd$ is very subtle, however, consisting of a relative difference of $\sim 10^{-3}$ in the tetragonal distortions of the oxygen octahedra around the iridium ions on each of the two sub-lattices. Although it has been shown that this structural distortion is important for the locking of the magnetic moment to the octahedral rotation[5], we believe that it should be of minimal importance for the calculated phonon dispersions. To show this explicitly, we have repeated the DFT calculations using the $I4_1/a$ structure from Ye *et al.*[6]. Figure S1 shows a comparison between the $I4_1/acd$ and $I4_1/a$ calculations. It can be seen that there is very little difference between the two, with shifts in the phonon energies well below the resolution of our IXS measurements.

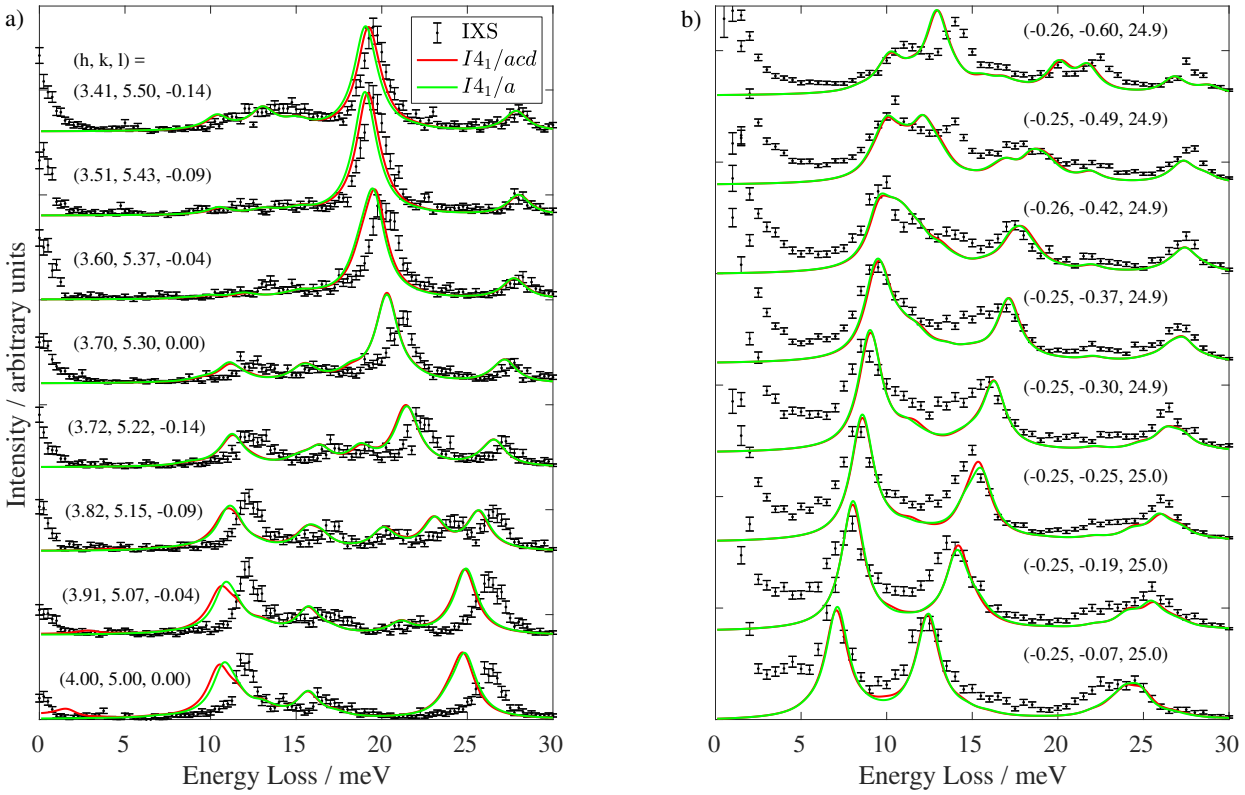

FIG. S1. Comparison of the DFT calculations for the $I4_1/acd$ (red lines) and $I4_1/a$ (green lines) space groups with the IXS data (black points) for a) the parent compound at 100 K and b) the doped compound at 9 K. All calculations were performed in the LDA approximation on a $2 \times 2 \times 1$ supercell.

III. COMPARISON WITH OPTICAL MEASUREMENTS

Here we compare our LDA calculation on the $2\times2\times1$ supercell with previously published Raman and infra-red (IR) spectroscopy studies. The primitive unit cell of Sr_2IrO_4 contains 28 atoms, giving 84 phonon modes. A symmetry analysis of the $I4_1/acd$ space group with Ir atoms at Wyckoff site $8a$, Sr at $16d$ and O at $16d$ (apical) and $16f$ (basal) shows that the Raman active modes have irreducible representations $3A_{1g}+5B_{1g}+4B_{2g}+13E_g$ and the IR modes have irreducible representations $5A_{2u}+13E_u$, leaving $4A_{1u}+4A_{2g}+4B_{1u}+3B_{2u}$. Table S1 shows that our calculated mode energies compare well to the Raman and IR studies.

LDA $2\times2\times2$			Ref. 7	Ref. 8 (Raman)		Ref. 9 (IR)	
Band	Assignment	Calculated	Calculated	Calculated	Observed	Calculated	Observed
1, 2	E_u	Acoustic	Acoustic	-	-	-	-
3	A_{2u}	Acoustic	Acoustic	-	-	-	-
4, 5	E_u	42	Imaginary	-	-	30	-
6, 7	E_g	56	Imaginary	-	-	-	-
8, 9	E_g	66	53	-	-	-	-
10, 11	E_u	80	84	-	-	81	103
12, 13	E_g	93	91	-	-	-	-
14, 15	E_u	103	101	-	-	92	115
16, 17	E_g	109	108	-	-	-	-
18	B_{1g}	123	114	110	-	-	-
19, 20	E_g	133	132	-	-	-	-
21, 22	E_u	135	120	-	-	122	138
23	B_{2g}	137	134	135	-	-	-
24	A_{1u}	137	-	-	-	-	-
25	A_{2g}	142	-	-	-	-	-
26	B_{1u}	142	-	-	-	-	-
27	B_{2u}	157	-	-	-	-	-
28	B_{1g}	179	167	168	-	-	-
29	A_{1u}	185	-	-	-	-	-
30	B_{2g}	185	173	-	-	-	-

31	A_{2u}	186	172	-	-	172	192
32, 33	E_u	189	174	-	-	178	-
34, 35	E_g	194	186	171	191	-	-
36, 37	E_u	197	194	-	-	186	-
38	A_{1g}	198	181	188	188	-	-
39, 40	E_g	213	203	-	-	-	-
41, 42	E_u	216	204	-	-	212	214
43, 44	E_g	224	205	-	-	-	-
45, 46	E_u	258	257	-	-	251	270
47, 48	E_g	276	266	-	-	-	-
49	B_{2u}	315	-	-	-	-	-
50, 51	E_g	315	291	-	-	-	-
52	A_{1g}	316	260	326	278	-	-
53, 54	E_u	319	293	-	-	298	283
55, 56	E_g	334	314	-	-	-	-
57, 58	E_u	340	314	-	-	323	324
59	A_{2g}	380	-	-	-	-	-
60	B_{1u}	381	-	-	-	-	-
61	A_{2u}	390	340	-	-	374	373
62	B_{1g}	409	359	391	-	-	-
63	A_{1u}	419	-	-	-	-	-
64	B_{2g}	419	371	410	395	-	-
65, 66	E_u	439	381	-	-	406	367
67, 68	E_g	439	380	-	-	-	-
69	A_{2u}	479	502	-	-	443	515
70	B_{2g}	491	513	457	495	-	-
71	A_{1u}	491	-	-	-	-	-
72	B_{2u}	503	-	-	-	-	-
73	B_{1u}	512	-	-	-	-	-
74	A_{2g}	512	-	-	-	-	-

75	A_{1g}	559	588	532	562	-	-
76	B_{1g}	576	596	546	-	-	-
77, 78	E_u	669	751	-	-	645	664
79, 80	E_g	670	751	-	-	-	-
81	B_{1g}	694	808	660	693	-	-
82	A_{2u}	694	808	-	-	660	-
83	B_{1u}	709	-	-	-	-	-
84	A_{2g}	709	-	-	-	-	-

TABLE S1: Comparison of the modes calculated with LDA on a $2 \times 2 \times 1$ supercell to those from previously published Raman and IR studies on Sr_2IrO_4. All frequencies are in cm^{-1}. The imaginary frequencies in Ref. 7 arise from their use of the unrelaxed experimental crystal structure.

IV. SUPPLEMENTAL DATA FOR THE PARENT AND DOPED SAMPLES

Here we present IXS spectra and LDA calculations on the $2 \times 2 \times 1$ supercell for the **Q** points indicated in Fig. **??** but not shown in the main text. The conclusions drawn in the main text (namely the good agreement between the experimental spectra and non-magnetic DFT calculations, and the lack of any visible anomalous frequency or linewidth changes through T_N) apply equally well to these data. Fig. S6 shows details of the fits of the doped spectra at 9 K and 250 K.

---

* cameron.dashwood.17@ucl.ac.uk

[1] A. Q. R. Baron, J. Spectrosc. Soc. Japan **58**, 205 (2009).

[2] A. Togo and I. Tanaka, Scr. Mater. **108**, 1 (2015).

[3] F. Ye, S. Chi, B. C. Chakoumakos, J. A. Fernandez-Baca, T. Qi, and G. Cao, Phys. Rev. B **87**, 140406(R) (2013).

[4] C. Dhital, T. Hogan, Z. Yamani, C. de la Cruz, X. Chen, S. Khadka, Z. Ren, and S. D. Wilson, Phys. Rev. B **87**, 144405 (2013).

[5] D. H. Torchinsky, H. Chu, L. Zhao, N. B. Perkins, Y. Sizyuk, T. Qi, G. Cao, and D. Hsieh, Phys. Rev. Lett. **114**, 096404 (2015).

[6] F. Ye, X. Wang, C. Hoffmann, J. Wang, S. Chi, M. Matsuda, B. C. Chakoumakos, J. A. Fernandez-Baca, and G. Cao, Phys. Rev. B **92**, 201112(R) (2015).

[7] K. Samanta, F. M. Ardito, N. M. Souza-Neto, and E. Granado, Phys. Rev. B **98**, 094101 (2018).

[8] H. Gretarsson, J. Sauceda, N. H. Sung, M. Höppner, M. Minola, B. J. Kim, B. Keimer, and M. Le Tacon, Phys. Rev. B **96**, 115138 (2017).

[9] D. Pröpper, A. N. Yaresko, M. Höppner, Y. Matiks, Y.-L. Mathis, T. Takayama, A. Matsumoto, H. Takagi, B. Keimer, and A. V. Boris, Phys. Rev. B **94**, 035158 (2016).

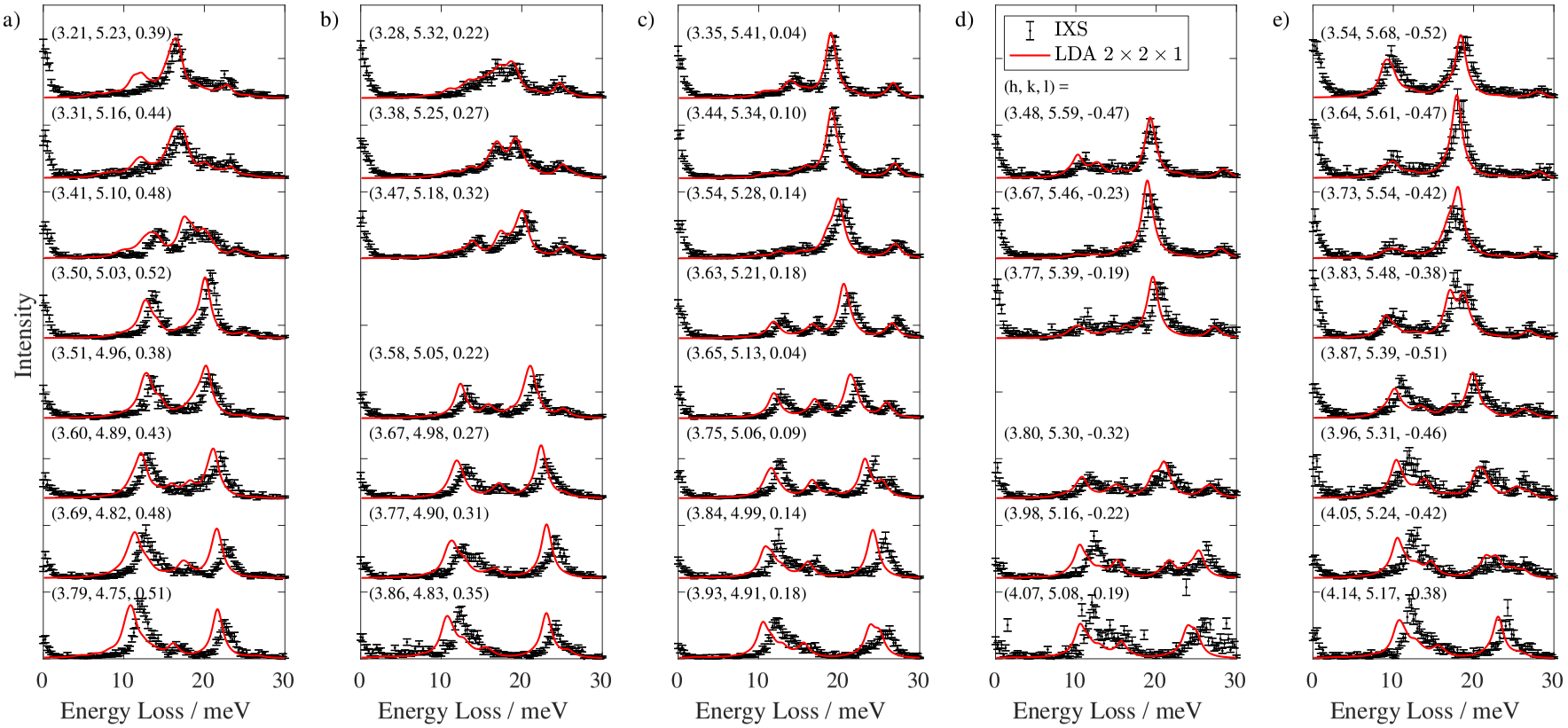

FIG. S2. IXS spectra in the parent compound at 100 K for each vertical column of analysers not shown in the main text (black points) compared to the dynamic structure factor calculated with LDA on a $2 \times 2 \times 1$ supercell (solid red lines). The spectra in each plot are offset vertically for clarity. The missing spectra are due to detector malfunctions.

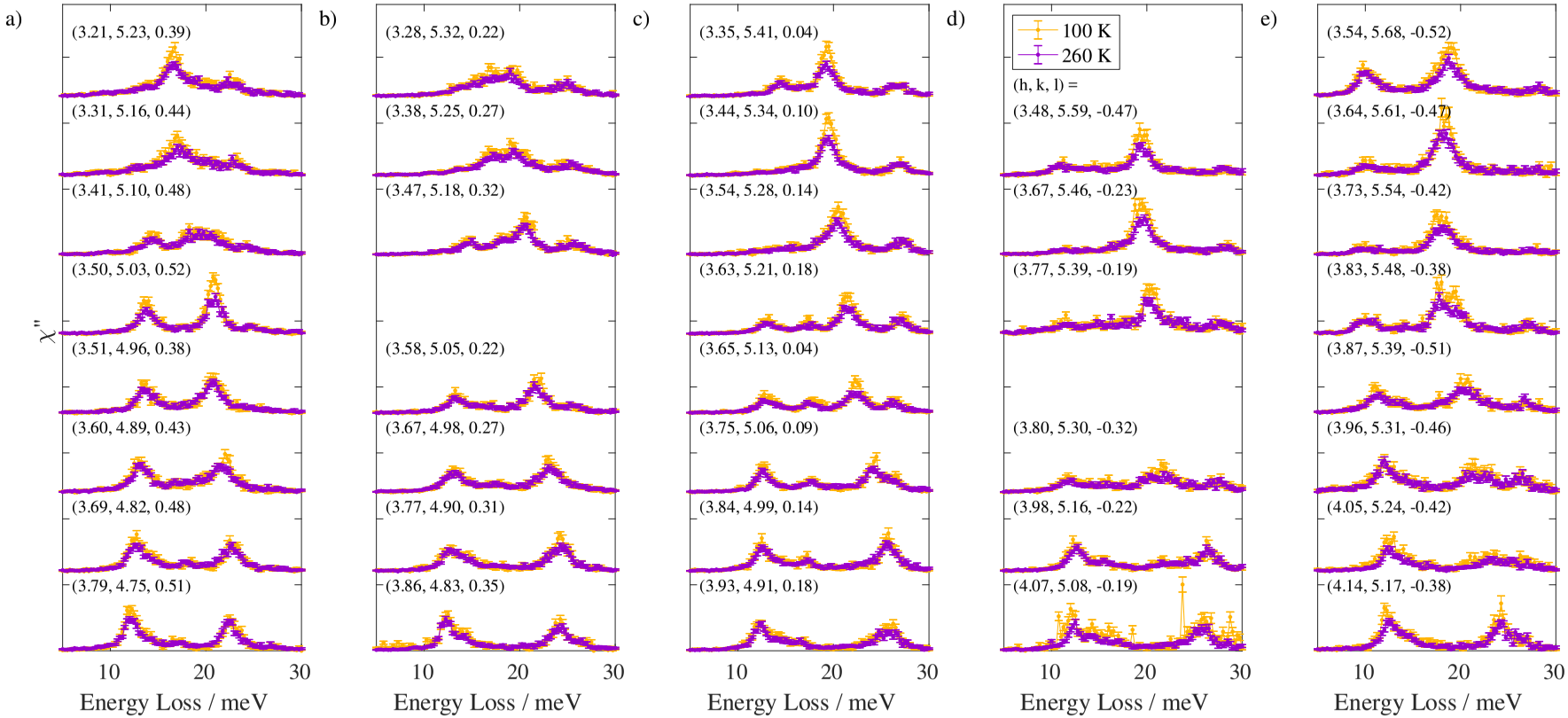

FIG. S3. Bose-factor corrected IXS spectra in the parent compound at 100 K (orange) and 260 K (purple) for for each vertical column of analysers not shown in the main text. The spectra in each plot are offset vertically for clarity. The missing spectra are due to detector malfunctions.

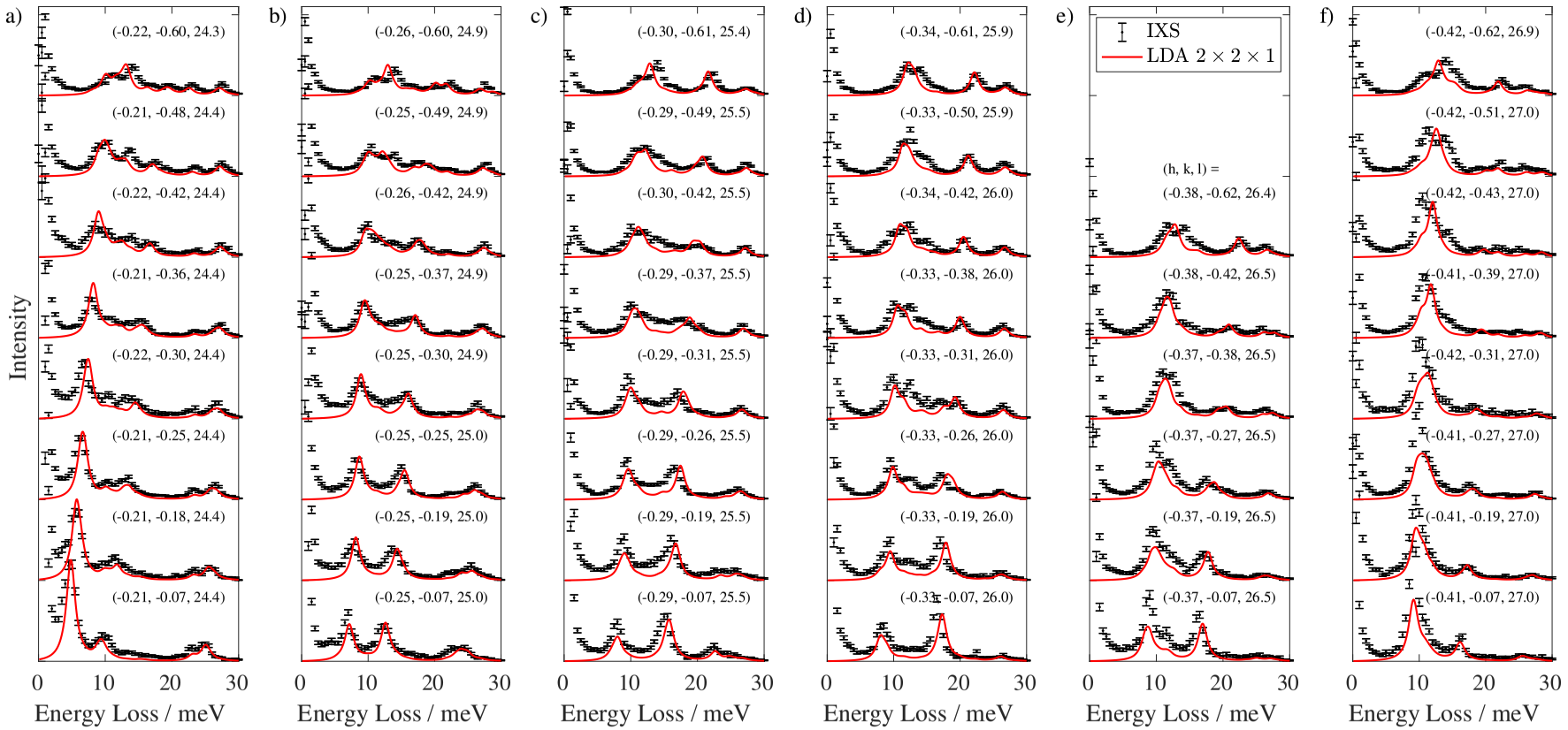

FIG. S4. IXS spectra in the doped compound at 9 K for each vertical column of analysers not shown in the main text (black points) compared to the dynamic structure factor calculated with LDA on a $2 \times 2 \times 1$ supercell (solid red lines). The spectra in each plot are offset vertically for clarity. The missing spectra are due to detector malfunctions.

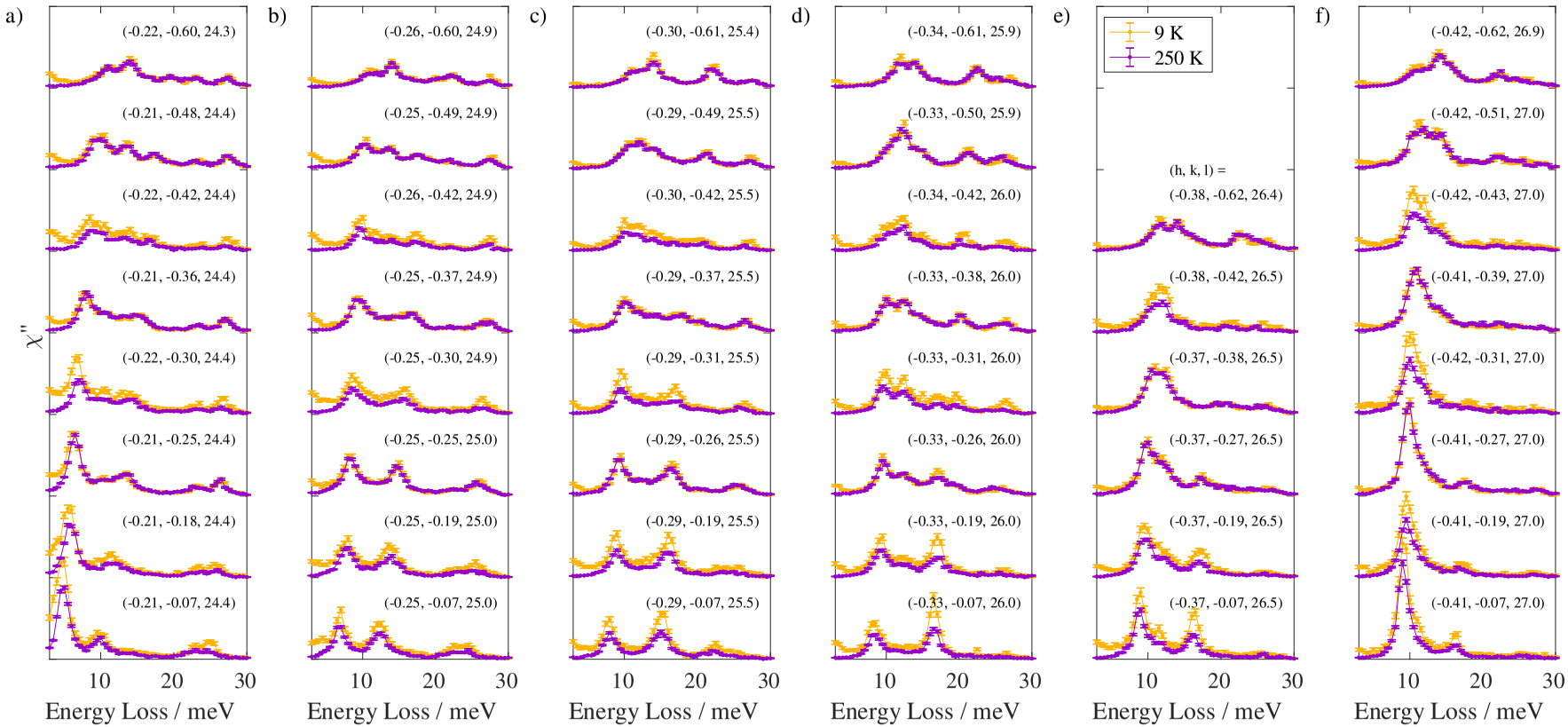

FIG. S5. Bose-factor corrected IXS spectra in the doped compound at 9 K (orange) and 250 K (purple) for for each vertical column of analysers not shown in the main text. The spectra in each plot are offset vertically for clarity. The missing spectra are due to detector malfunctions.

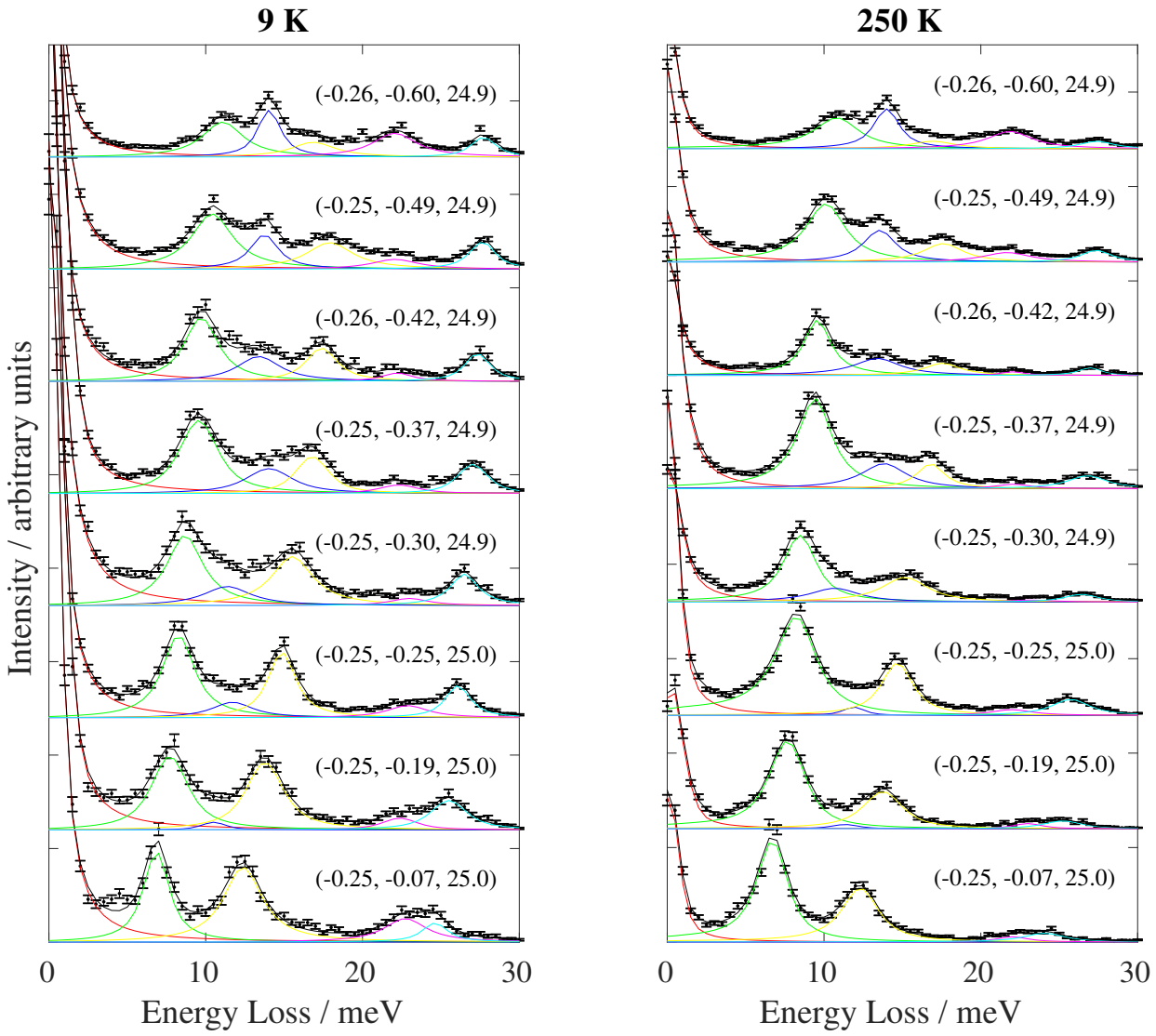

FIG. S6. Detail of the fits (black line) of the doped spectra (black points). As described in the main text, the elastic peak is fitted with a pseudo-Voigt resolution function (red), while each of the phonon modes is fitted with a damped harmonic oscillator lineshape weighted by the Bose factor and convoluted with the resolution function (green, blue, yellow, magenta and cyan respectively for each mode).